

Fatigue crack analysis of ferrite material by acoustic emission technique

Md. T. I. Khan^{1*}, A. A. Rashid¹, R. Hidaka¹, N. Hattori² and Md. M Islam³

¹Department of Advanced Technology Fusion, Saga University,
1 Honjo-machi, Saga 840-8502, Japan
Phone: +81-952-28-8628, Fax: +81-952-28-8587
*E-mail: khan@me.saga-u.ac.jp

²Department of Mechanical Engineering, Saga University,
1 Honjo-machi, Saga 840-8502, Japan

³School of Mechanical and Electrical Engineering, University of Southern Queensland,
West St, Toowoomba, QLD 4350, Australia

ABSTRACT

Among various methods of Non-destructive techniques (NDT), analysis using released acoustic emission (AE) waves due to crack propagation is very effective due to its dynamic monitoring features. In fragmentation theory for AE there are some proportional relationships among the AE parameters i.e. AE event, AE energy, area and volume of cracks etc., which are calculated from the released AE waves from the dynamic crack inside any material. The necessity of calculating the fractal dimension has been found in such relationships and the value is emphasized for determining the geometry of the irregularity in crack surface and crack volume. In this paper a novel approach for evaluating that value based on image processing by MATLAB is proposed. The images of the cracks during propagation are preserved and utilized to find out the fractal dimension for analyzing the crack propagation characteristics. The AE energy is also estimated from the received AE waves. The positioning of the sensors plays a great impact on this calculation. Finally, the theoretical proportionality relations of AE parameters are interpreted experimentally during crack propagation behavior in ferrite cast iron under fatigue loading.

Keywords: Acoustic emission; acoustic energy; ferrite material; fatigue loading; fractal dimension; image processing.

INTRODUCTION

With the advancement of time, the processes of actuating the formation and propagation of cracks are still the object of in-depth research as it allows the prevention of fatal effects of the materials and forecasts the causes of failure [1]. There are various Non-destructive techniques (NDT), like eddy current inspection, liquid penetrant inspection and ultrasonic methods, available to measure and check the progression of detrimental structural conditions [2, 3]. Among all the NDTs, the acoustic emission (AE) technique is proved very effective and it is widely used now for damage identification and characterization [4]. AE technique utilizes AE waves which are easily received during the damage of material using sensors and

the assessment setup is much simpler as well. Moreover, from the AE signal analysis information on the cracking modes or the assault of a crack can be obtained [5, 6]. Among all the available methods of NDT, AE technique is the mostly known method to be utilized as a dynamic damage detection technique in the aspect of damage characterization and crack propagation monitoring [7-9].

When a crack is formed in any material, it propagates due to the loading condition on the material and afterwards, the material is fractured within its cracking period as well. During crack propagation, the molecular bonds are ruptured, releasing small amounts of energy. The released energy advances throughout the surrounding material in the form of stress waves. Usually, all structural changes release some form of energy into the material, resulting in waves similar to those of the crack growth. The acoustic emission technique consists of piezoelectric sensors which are used to transform the elastic transient waves to electrical signal [10]. These waves are produced by the sources, such as crack propagation or impact, within the structural material under study. In our experiment a crack was formed by applying fatigue loading on the material. So this is the dominant cause for the formation of AE waves. The AE waves, due to crack propagation, were received from this phenomenon and processed as the amplitude (voltage) vs time (second) data. From this data different parameters of the AE waves were determined [11]. A sample of AE signal is shown in Figure 1 with its various considerable parameters.

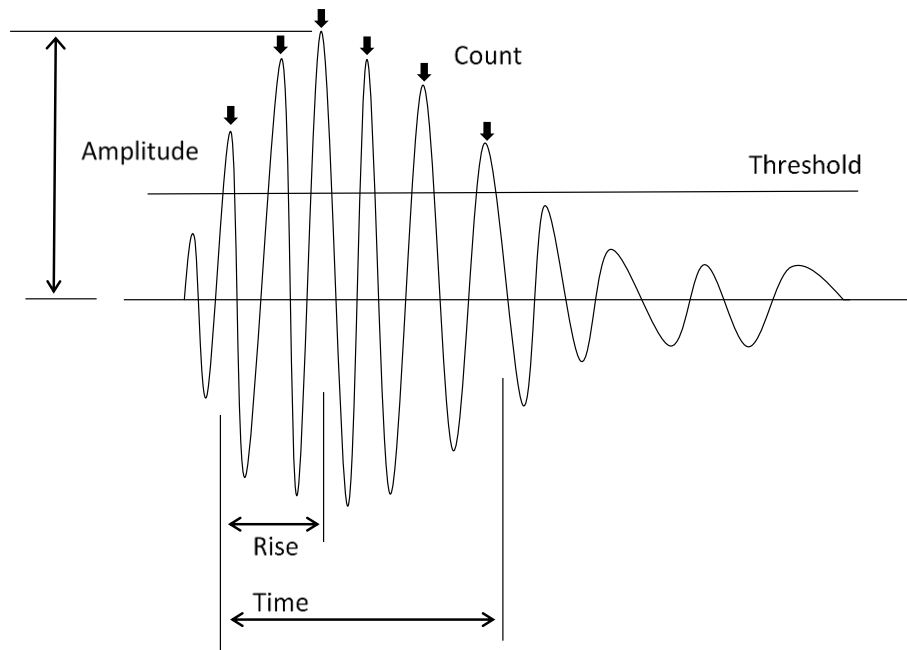


Figure 1. An AE signal with different parameters.

All the above parameters have different characteristic meanings. Among them, AE energy is very important as it shows the fragmentation level of a crack in a material effectively and also can be used for the analysis of the AE source [12]. It reflects the received energy of AE signal. The energy is released during the elastic deformation. But it is emitted at a higher rate during the deformation of a material at two stages. One is during the plastic

deformation, and the other when the fracture occurs [13]. In this paper, AE energy was evaluated by dividing the summation of squared values of AE signal amplitude by the AE signal duration (as shown the parameters in Figure 1). Utilizing the fragmentation theory, there are some proportionality relationships formulated between the crack region and the AE energy released during the crack development [14].

Recently, the fragmentation theory has been investigated on quasi brittle materials under compressive loads [15]. In this paper, emphasis is given to show material (ferrite) behaviors under fatigue loading conditions. Collecting the AE data during the whole cracking process, from formation until breakage, it is shown that AE energy is related with crack propagation using fragmentation theory. In the theory there are some other parameters like fractal dimension of the crack region. There are various methods available to determine that parameter [16]. But in this paper a new approach is proposed for finding the fractal dimension of a crack surface or volume. This method utilizes MATLAB image processing tool box for the calculation, and it is found that it has much more advantages in easy calculation method as well as less calculation time compared to the most well-known box counting method. By our algorithm, area and volume of the crack region are also found out at the same time of finding the fractal dimension. Crack volume and crack area are used to show their influences on the AE energy and AE events which are obtained from the ferrite material due to crack propagation. Thus, these relationships among them will work as an extensive step in relating the AE wave nature with damage characterization [17].

THEORY

AE Event

Due to application of fatigue load on the material, crack is developed at a certain time and it continues which causes AE waves to form and transmitted through the material. These AE waves are received by the sensors placed on the surface of the material. These are individually known as AE event and the total number of AE events from initiation to termination is denoted by N.

AE energy

Acoustic emission activity is associated with the rapid release of energy in a material. The acoustic energy is directly proportional to the area under the acoustic emission waveform [18]. In order to determine this parameter, the following Eq. (1) is used for the experimental analysis:

$$E = \frac{1}{T} \sum_{i=1}^n A_i^2 \quad (1)$$

where, E is acoustic energy, A is the amplitude of a AE signals above the threshold value and T is the duration as shown in Figure 1.

Energy Relations of AE in Fragmentation Theory

The energy during crack propagation is released due to crack formation and friction between the crack surfaces. The fragmentation theory is based on the AE energy produced due to fragmentation of any volume of material. From fractal fragmentation theory, it can be shown that the AE energy developed due to crack is related with the surface and volume of the crack. The relationship among them is shown by Eq. (2) as follows [19].

$$E \propto A_C \propto V_C^{D/3} \quad (2)$$

where E is the released AE energy from the crack region, A_C is the total crack surface area and V_C is the total volume of crack region. D is the fractal dimension and a very important factor for characterizing the nature of the fragmentation. Sudden failure causes the value of D near to 2 where large area damage makes that value near to 3. So the value ranges from 2-3 [20]. The AE energy release E is also proportional to the number of AE events N during micro crack propagation and written by Eq. (3) as follows:

$$E \propto N \quad (3)$$

The fractal criterion can be rewritten using the Eq. (2) and (3) as follows:

$$E \propto N \propto A_C \propto V_C^{D/3} \quad (4)$$

The theoretical expression as shown by Eq. (4) is explained and verified in our AE experiments on cast iron (ferrite) under fatigue loading and showed the conservation of the theoretical relations with the experimental approach.

Fractal Dimension Analysis

In the fragmentation theory discussed above, one of the parameter of calculation is fractal dimension. It is a very important geometric property of a body. When there is an irregular body, it becomes difficult to find the dimension of that body and the value is not always a natural number. So the concept of the fractal dimension is introduced (by Mandelbrot, 1982) to find the fractional dimension of any irregular shape [21]. The fractal dimension gives an idea of the complexity of the object. The theory of finding the fractal dimension depends on the concept of self-similarity. Usually the irregular body does not have a particular simple form. So the scale of measurement is divided into small pieces so that it can cover the original form [22]. The equation of finding the fractal dimension (known as Felix Hausdorff dimension) is given below by Eq. (5):

$$C = y^D \quad (5)$$

From where the relation is derived and shown by the Eq. (6) as follows:

$$D = \log C / \log y \quad (6)$$

where C is the total number of copies of the small pieces needed to cover the whole body and y is the number of similar identities a standard length is divided into. The variation of the values of C and y for 1D, 2D and 3D are shown in Figure 2. When the values of C and y are put in Eq. (6), the fractal dimension of Figure. 2. (a), (b) and (c) become equal to 1, 2 and 3 respectively and thus these values show the dimensions of the figure respectively. This is the primary concept of fractal dimension analysis.

Box Counting Method

Among the available methods, determination of fractal dimension by box counting is more popular for its effectiveness in calculating the fractal dimension of the complex body [23]. In this case the ratio of the log of the number of non-empty box is taken with the log of the number of grid in one direction.

First the whole image is considered, then with each iteration the box size is decreased by a factor of two and thus plotting all the values for each iteration the slope of the common line by this points is considered as the fractal dimension [24]. There is a disadvantage of this method which we faced during our calculations, that this method is simple for 2-D body but when 3-D is considered the number of box count increases at a very high rate which requires more memory to store box counts and thus the calculation cost increases rapidly [25]. Most of the time the program crashes before achieving the accurate result (although it depends on the capacity of the computer). In order to solve this problem, a new method of finding the fractal dimension is proposed.

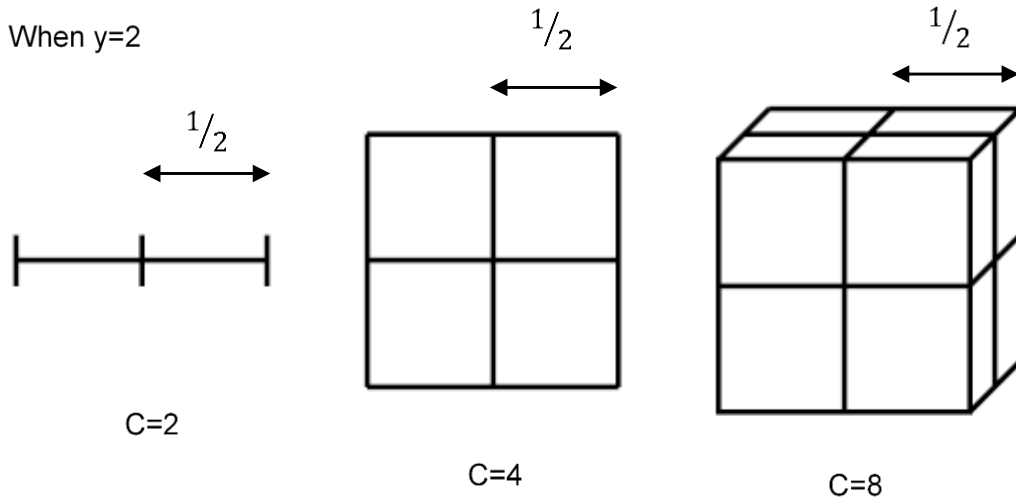


Figure 2. Concept of fractal dimension

Proposed Method

In this research, MATLAB program has been created for the analysis of fractal dimensions based on image processing algorithm. In the proposed calculation, y_0 is considered as the number of pixels in unit length of 1 mm and C is the number of pixels per square or volume of the figure for which fractal dimension is to be found. To avoid the complexity of irregularity of the shape of crack, we take the unit length as the standard length. Then we divide it to the smallest pieces in pixels. The equation for calculation of fractal dimension becomes as Eq. (7):

$$D_m = \log C / \log y_0 \quad (7)$$

where D_m is the fractal dimension of any shape by the proposed method, $\log C$ is the logarithmic value of the number of pixels per square or volume of the shape and $\log y_0$ is the logarithmic value of the number of pixel in unit length of 1 mm.

EXPERIMENTAL METHODOLOGY

Specimen Details

For conducting the fatigue experiment noted in this paper, the cast iron (Ferrite) is used. Ferrite is a ductile cast iron. Figure 3 below shows the dimensions of the specimen used and the mounting position of four sensors used in the experiment. The four sensors' positions are shown by CH1, CH2, CH3 and CH4. The thickness is 5 mm. There is a circular perforation in the middle of the specimen and that portion is made slender in order to narrow down the location of the crack formation for easy inspection. The physical and mechanical properties of the specimen are given in the Table 1:

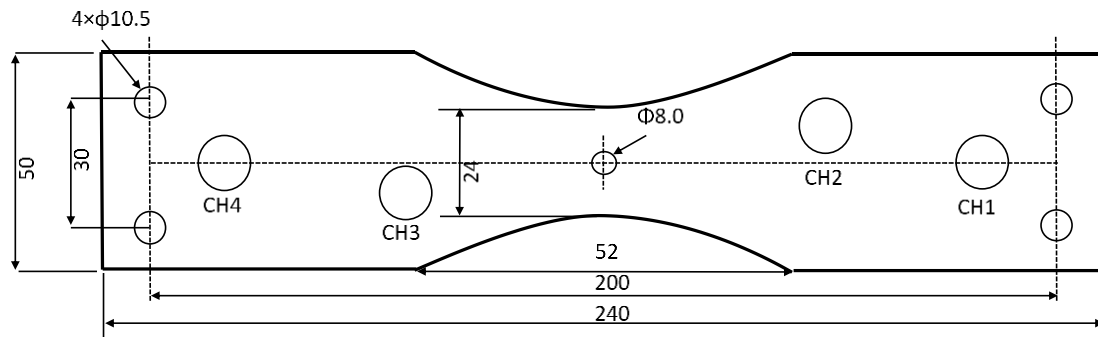


Figure 3. The dimensions and the mounting positions of sensors of the ferrite specimen.

Table 1. The properties of ferrite.

| Material name | Tensile strength [MPa] | Elongation [%] | Hardness [HBW] | Particle density [pieces/mm ²] | Graphite rate [%] | Perlite rate [%] | Ferrite rate [%] |
|---------------|------------------------|----------------|----------------|--|-------------------|------------------|------------------|
| LDI-L-AE | 390 | 23.8 | 137 | 58.3 | 20.2 | 3.3 | 96.7 |

Fatigue Loading Machine

The Servo Pulser machine is used to give the fatigue loading on the specimen to create crack inside the body until it is ruptured. The specifications of the machine are provided in the table 2:

Table 2. The major specifications of Servo Pulser.

| | | |
|--------------------|----------------------|---|
| No. | 37937 | |
| Manufacturer | SHIMADZU Corporation | |
| Type | EHF 10U | |
| Date | March 1977 | |
| Controller model | 4836 | |
| Measurement target | Load, stroke | |
| Loading waveform | Standard types | Sine wave, haversine wave, triangle wave, rectangular wave, ramp wave and hold wave |
| | Frequency | 0.001 Hz to 1000 Hz |
| Load amp | Adaptive detector | Strain gauge type load cell |
| | Range | $\pm 150 \pm 100 \pm 50 \pm 20, \pm 10$ |
| | Rated Output | $\pm 5V$ for each range full scale |
| Stroke Amplifier | Conformity | Differential transformer type displacement gauge etc. |
| | Range | $\pm 150 \pm 100 \pm 50 \pm 20, \pm 10$ |
| | Rated Output | $\pm 5V$ for each range full scale |

Experimental Procedure

The whole setup was assembled according to the schematic diagram shown in Figure 4. 40% of the tensile strength and the area of the loading surface of the specimen were taken into account for the determination of the initial load. By calculating the fatigue test was set with an initial load of 11.5 kN, an amplitude of load of 11.5- 21 kN and a loading frequency of 10Hz. Loading waveform was selected as sine wave. First the primary load was set by the Servo Pulser controller. Four AE sensors (R15-ALPHA), preamplifier (Model 2/4/6, 28VDC-0.2A) having voltage gain 40dB, AE amplifier and oscilloscope (Model TDS2024B) were connected to the test piece. The starting time of the oscilloscope and PC were recorded and the test was started.

When AE event was detected, the set up was stopped and the data regarding the received event from the oscilloscope was saved. This is called a AE hit. During the process when crack was visible on the surface of the specimen, a replica of the crack was made at the time of collecting the data from the AE hit. Testing was continued until the specimen was broken. All the information was collected for the analysis. In the oscilloscope, the horizontal axis was considered as time, where 1 unit was equal to 250 μs (sampling frequency of 1MHz) and the vertical axis was considered as voltage, where 1 unit was equal to 1.00 V. CH2 was assigned as the triggered channel. In order to eliminate noise such as vibration noise of the testing machine when calculating the AE data, the threshold value was calculated as 0.08 mV. In this experiment there were a total of 88 AE events collected before the specimen was ruptured and the replica of the specimen surface of 67th, 72nd, 77th, 82nd and 87th events were collected.

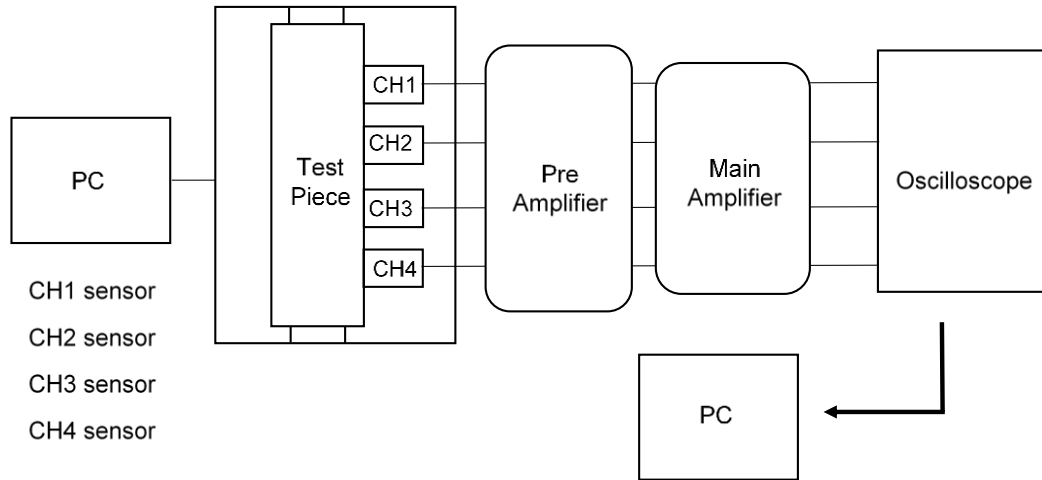


Figure 4. Schematic diagram of the experimental setup.

EXPERIMENTAL RESULTS AND DISCUSSION

Fractal Dimension Calculation

In order to confirm our proposed method of finding fractal dimension, at first we compare it with the known fractal dimensions of some common images. For that purpose, we took square, Koch curve and Sierpinski gasket. The fractal dimensions of these images are determined both by box counting method and our proposed method. The comparisons are as follows in Table 3. With our proposed method we get errors of 0%, .74% and 2.7% for the three figures respectively and the errors are minimum. Thus our approach is verified for fractal analysis of the specimen as well.

Table 3. The values of D_t , D_b and D_m for Square, Koch Curve and Sierpinski gasket

| | Square | Koch Curve | Sierpinski gasket |
|-------|--------|------------|-------------------|
| D_t | 2.000 | 1.268 | 1.585 |
| D_b | 2.000 | 1.268 | 1.592 |
| D_m | 2.000 | 1.2754 | 1.612 |

Here, D_t , D_b and D_m are the true values, box counting values and our proposed method's values of the fractal dimension respectively.

In order to find the fractal dimension of the crack, the microscopic views of the replicas of the crack is considered. Replicas of the crack were taken when the number of events were 67, 72, 77, 82, 87. This is due to the fact that after 66th events, the cracks were much visible on the material surface and on the replica surfaces as well with a satisfactory crack profiles. There were some gaps among the events due to the consideration that the crack profiles were almost same in the missing events. During the calculations all the major and dominating cracks were considered. The microscopic image of the replica for the crack of 87th event is shown in Figure 5.

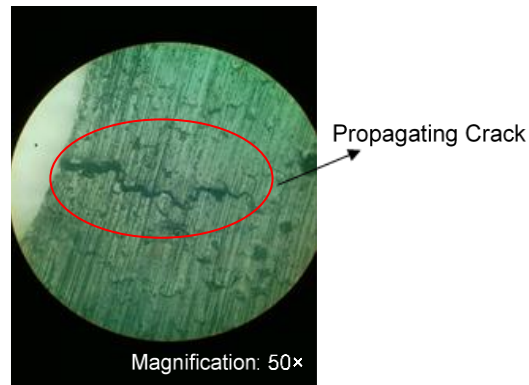


Figure 5. Microscopic view of the replica of 87th AE event (50x magnification).

According to the proposed technique, first the part of the crack needed to be considered was trimmed, from the received microscopic image of the replica, by using MATLAB. Then a binary image of that selected image was made and the fractal dimension of the crack region was determined. The selection and conversion of the selected image prior to calculation is shown below in Figure 6.

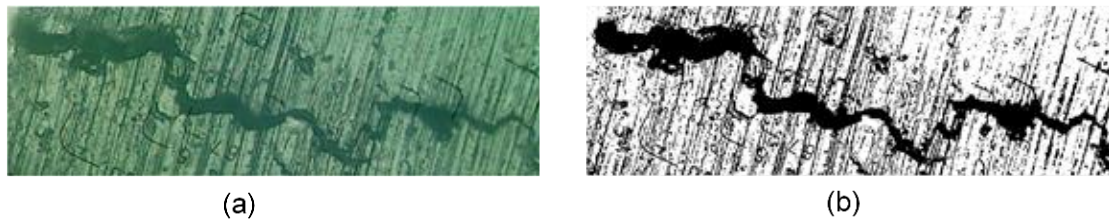


Figure 6. Step by step crack analysis, (a) selection of the region containing the dominating crack, (b) binarization of the selected region.

To get the fractal dimension of the crack volume, it was assumed that crack is formed thorough the depth as uniform fatigue loading was provided. The algorithm of the above proposed image processing for calculating the fractal dimension related to crack propagation is summarized as Fig. 7.

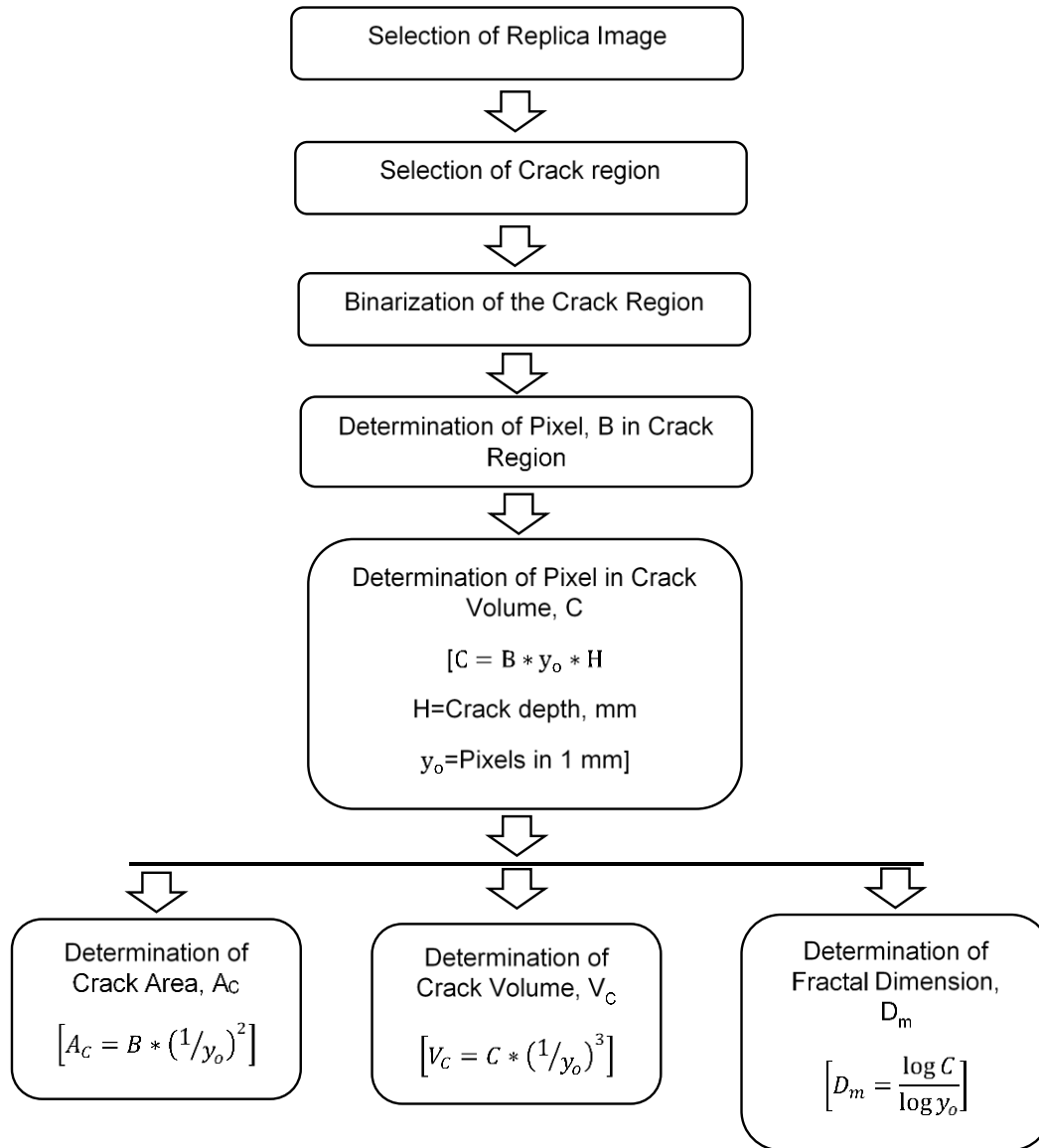


Figure 7. The flow chart of the algorithm of the proposed fractal dimension analysis method.

Replicas of AE events 67, 72, 77, 82 and 87 were taken for the study of crack propagation as from 66th event and afterward the cracks were visualized more certainly on the surface. As the number of AE events increases the crack becomes larger and thus the crack area and volume increases. The value of calculated fractal dimension by both using the proposed method and the box counting method and the determined value of the crack area and volume are given in Table 4.

The comparison is also shown in the form of graph in Figure 8. The error between the two methods is higher (less than 7%) due to the reduction of the number of iteration (65 iteration) in case of box counting to prevent program crashing. From the graph for both

methods the average trend of increasing of fractal dimension with the increase of the AE events are seen.

Table 4. Fractal dimensions, the areas and volumes of the cracked region.

| Number of AE Events N | Fractal Dimension | | Percentage Error % | Area A_C [mm ²] | Volume V_C [mm ³] |
|--------------------------|-------------------|--------|--------------------|-------------------------------|---------------------------------|
| | D_m | D_b | | | |
| 67 | 2.5178 | 2.3879 | 5.43993 | 0.00000252633 | 0.000015158 |
| 72 | 2.4058 | 2.5772 | 6.650629 | 0.00000307683 | 0.000018461 |
| 77 | 2.7458 | 2.7632 | 0.629705 | 0.0000141537 | 0.000084922 |
| 82 | 2.8273 | 2.6879 | 5.1862 | 0.000266667 | 0.0016 |
| 87 | 2.9553 | 2.845 | 3.87698 | 0.009033333 | 0.0542 |

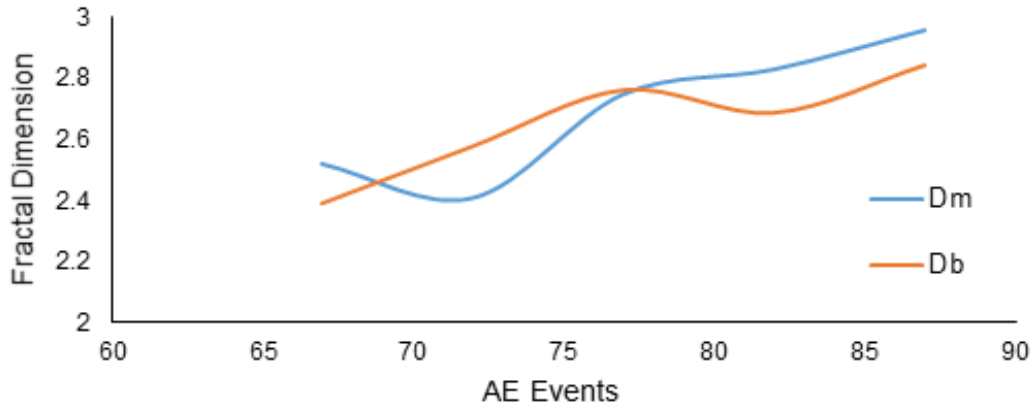


Figure 8. Comparison between D_b and D_m .

Damage Characteristics using AE Energy with AE Events

The values of AE energy and AE event number were calculated from the AE data received from the experiment and their relationships are shown. The calculated result of AE energy, E and AE event number, N are shown by Figure 9. The whole region is divided into 4 distinctive regions comparing with the regimes of primary growth rate mechanisms shown by Ritchie (1977) [26]. The proportional relationship from 0th to 52th events due to elastic deformation and formation of micro crack inside the body are shown from the graph of E and N. The crack was not visible on the surface of the material so the evidence of the micro cracks is verified. The region is shown in the Figure 9 and named as CR1, but there is a sharp rise at 37th event. This is thought to occur due to the sudden release of AE energy of a major crack inside the body. This phenomenon is rare and the cause is due to the impurities distribution inside the material. In 52th to 62th events there is a rise of the AE energy and it is specified as CR2. During this stage the plastic deformation starts thus the release of the AE energy is higher. In 62th to 76th events, there is a proportional relationship and named as CR3. The slope of CR3 is less than the slope of CR2 but constantly rising. During this stage crack starts to visualize on the surface of the specimen. Then after 76th event the rise of AE energy is the

highest and finally the body is fractured after 87th event. This region is named as CR4. Since CR1 is dominated by the elasticity of the material, the hypothesis of Ritchie can be considered from CR2-CR4 and it shows the same trend. Thus fatigue growth rate can be illustrated by the graph of E vs N and the relation, $E \propto N$, received from the fragmentation theory, cannot be shown throughout the crack propagation as there are lots of phase changes in cracks during the process until fragmentation. It does not remain constant for the whole period but it remains constant for CR1, CR2, CR3 and CR4 regions.

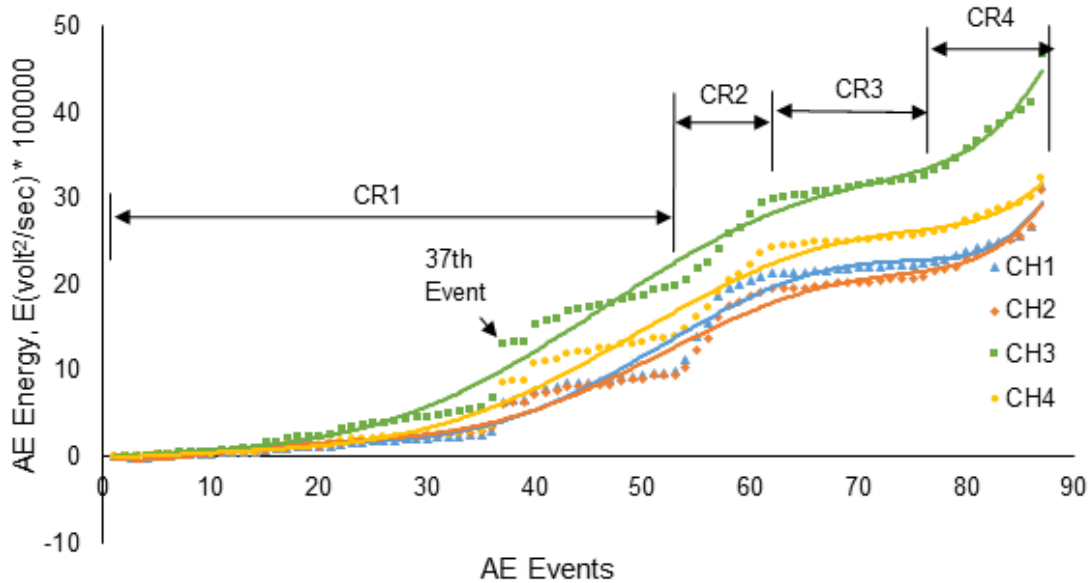


Figure 9. Graph of AE energy, E and AE events, N .

Damage Characteristics using Crack Area and Volume with AE Energy and AE Events

The values of crack area and crack volume and the fractal dimension were all calculated using the proposed program and compared with AE energy and AE events to observe the relationship among those parameters. Figures 10a, 10b, 11a and 11b are the graphs using the experimental results from the AE event number N greater than 66 because the crack could not be seen on the surface of the material using the microscope in the previous AE events. The first two graphs of Figure 10 show the relationship of AE energy E with crack volume, V_C and crack area, A_C . From the beginning the proportional relationship prevails with the propagation of crack which is shown by the red circles. The value looking like constant is due to very miniscule increment (according to Table 4) of both crack area and crack volume in the initial stage. So it is not observed in the graph so clearly. Just before the fragmentation the crack area as well as crack volume became largest and the energy released from the crack was largest as well. This kind of sudden growth of the fracture area and volume and the rise of AE energy at the same moment were observed during the experiment from the specimen and the result was also illustrated in the graph very clearly by an exponential rise. Thus the idea of rupture point for the material can be received from this graph.

Same conclusions are achieved as above and shown in Figure 11a and 11b, based on the graphs of AE events N with A_C and $V_C^{D/3}$. From here we see that around 80th event the curve rises exponentially from all the readings of the four sensors. The proportionality

relation until the 80th event is shown by a red circle. Since N is the same for every sensor, all the data received from the four sensors are shown by one curve.

The data collected from four sensors are shown from Figure 8 and Figure 9 the. Variation of data from the four sensors were found. At first the values were same but it started to vary as the AE event increases according to Figure 8. Figure 3 shows the position of the four sensors used on the specimen. CH1 and CH4 were near to the machine attachment zone and CH2 and CH3 were near to the crack formation region as the specimen was made in such a way that the crack would be formed in the center. During the experiment the fatigue load was given at the top and CH1 was near to that point. Thus it contained the most of the noises from the machine than CH4. CH2 and CH3 received most of the AE wave as those were near the crack propagation region. But for the case of CH2 it was affected by the machine noise of CH1 and thus the readings were decreased. The AE wave received by CH4 was also decreased due to the propagation of the wave inside the material and also for the remaining machine noise. All these facts affected the data of four sensors and caused the major variations. These are easily observed from the graphs of Figures 9, 10a and 10b.

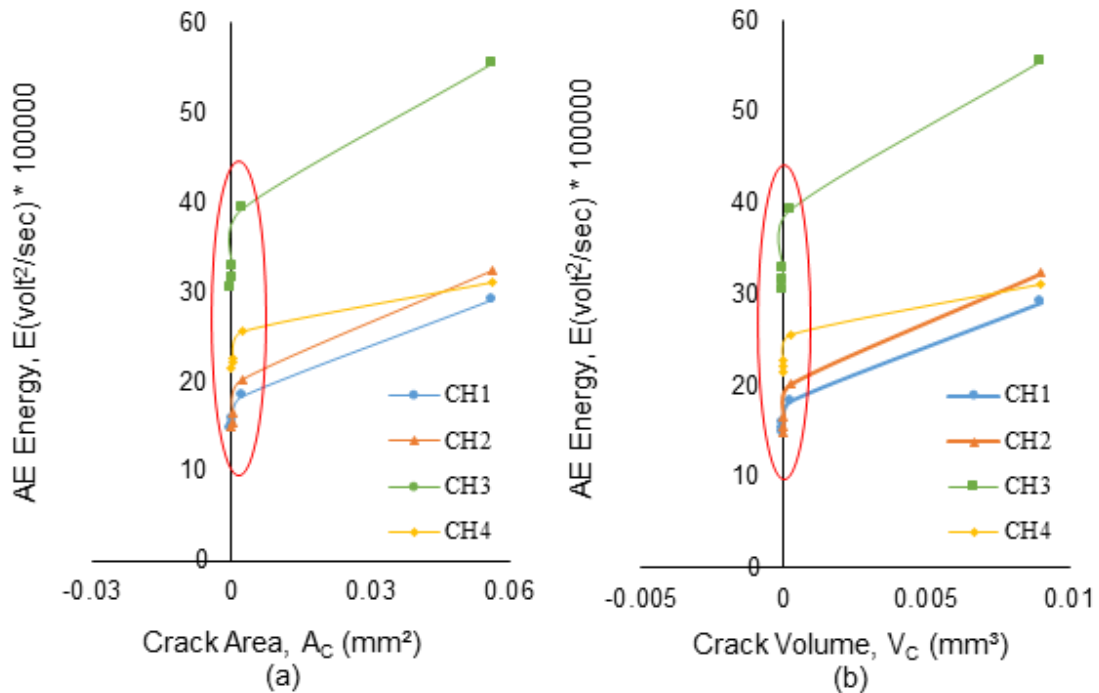


Figure 10. Graphs of (a) AE Energy, E and crack area, A_C and (b) AE Energy, E and crack volume, $V_C^{D/3}$.

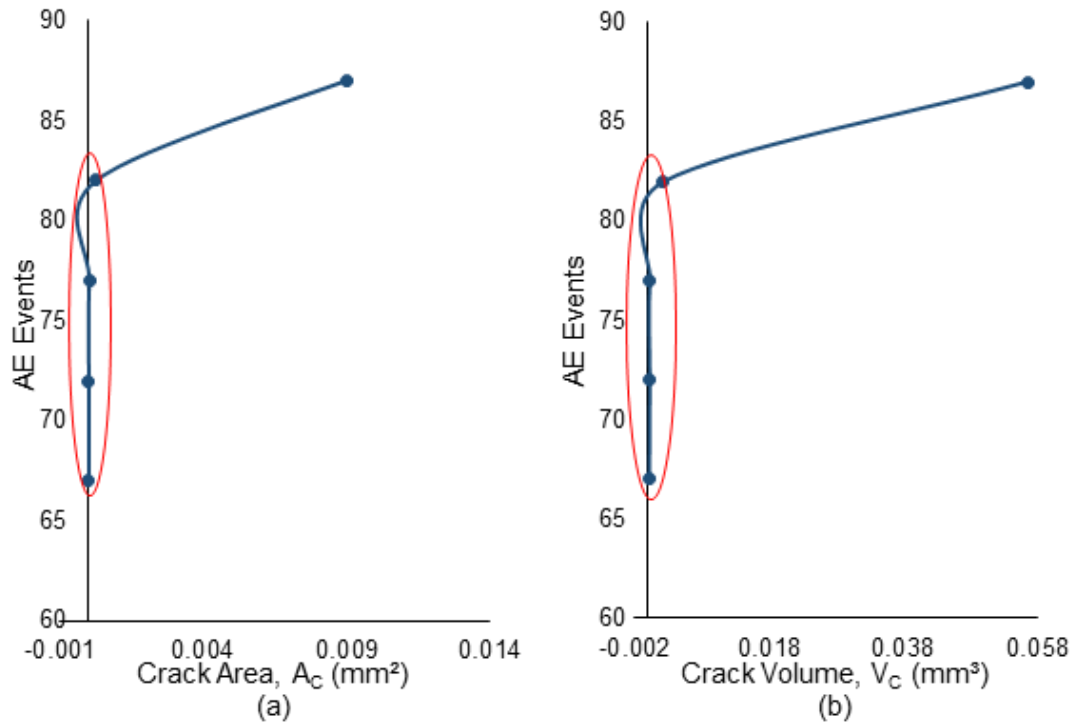


Figure 11. Graphs of (a) AE Events, N and crack area, A_C and (b) AE Events, N and crack volume, $V_C^{D/3}$.

CONCLUSIONS

The present experimental study demonstrates clearly the fragmentation theory for crack propagation due to fatigue loading condition in the material. The proportionality relations among acoustic emission events (N), acoustic emission energy (E), crack area (A_C) and crack volume (V_C) are clarified in details and shown in graphical representation using the calculated data received from the experiments. Although the proportionality relations do not prevail constant the whole period however it is proved that this relation exists similar for individual regions of cracking. In the relation of AE energy and AE events, 4 distinctive regions were shown where the proportionality relationship prevails. Sudden rises are observed besides the proportionality relationship of crack area and volume with AE energy and AE Events. These give a clear idea about the rupture points in the material cracking.

For finding the above relations of AE parameters with crack propagation the fractal dimensions (D) were calculated based on our proposed image processing technique. Our calculation results are compared with box counting method and found less calculation errors are found. Therefore, the trend of the proportionality relations among the AE parameters and crack volume becomes constant.

From the damage characteristics graph a variation of data were gotten from four sensors. This is mainly due to the machine noise produced during the application of load. Loading was applied near CH1 so it received most of the noises and this also influenced CH2

data. CH3 received most of the AE wave and thus the reading is higher and more accurate. CH4 received the remaining noise and thus show the little bit less reading than CH3. In this paper the whole process is shown for ferrite and under fatigue loading only. But this method is being applied now on other materials under different loading conditions as well. This whole method can be used as a good assessment tool for other materials in different conditions.

REFERENCES

- [1] Kotowski P. Fractal dimension of metallic fracture surface. *International Journal of Fracture*. 2006;141(1-2):269-286.
- [2] Carpinteri A, Lacidogna G. Structural Monitoring and Integrity Assessment of Medieval Towers. *Journal of Structural Engineering*. 2006;132(11):1681-1690.
- [3] Riemer A, Leuders S, Thöne M, Richard HA, Tröster T, Niendorf T. On the fatigue crack growth behavior in 316L stainless steel manufactured by selective laser melting. *Engineering Fracture Mechanics*. 2014;120:15-25.
- [4] Strantza M, Van Hemelrijck D, Guillaume P, Aggelis DG. Acoustic emission monitoring of crack propagation in additively manufactured and conventional titanium components. *Mechanics Research Communications*. 2017;84:8-13.
- [5] Aggelis DG. Classification of cracking mode in concrete by acoustic emission parameters. *Mechanics Research Communications*. 2011;38(3):153-157.
- [6] Yonezu A, Arino M, Kondo T, Hirakata H, Minoshima K. On hydrogen-induced Vickers indentation cracking in high-strength steel. *Mechanics Research Communications*. 2010;37(2):230-234.
- [7] Aggelis DG, Kordatos EZ, Matikas TE. Acoustic emission for fatigue damage characterization in metal plates. *Mechanics Research Communications*. 2011;38(2):106-110.
- [8] Kordatos EZ, Aggelis DG, Matikas TE. Monitoring mechanical damage in structural materials using complimentary NDE techniques based on thermography and acoustic emission. *Composites Part B: Engineering*. 2012;43(6):2676-2686.
- [9] Roberts TM, Talebzadeh M. Acoustic emission monitoring of fatigue crack propagation. *Journal of Constructional Steel Research*. 2003;59(6):695-712.
- [10] Berlinsky Y, Rosen M, Simmons J, Wadley HNG. A calibration approach to acoustic emission energy measurement. *Journal of Nondestructive Evaluation*. 1991;10(1):1-5.
- [11] Obaidi SMAA, Leong MS, Hamzah RIR, Abdelrhman AM, Danaee M. Acoustic emission parameters evaluation in machinery condition monitoring by using the concept of multivariate analysis. *ARNP Journal of Engineering and Applied Sciences*. 2016;11(12):7507-7514.
- [12] Dong D, Xiangdong Z, Libin L. Research on relationship between parameters correlation of acoustic emission and rock failure. *Sensors and Transducers* 2014;183(12):147-154.
- [13] Kral Z, Horn W, Steck J. Crack propagation analysis using acoustic emission sensors for structural health monitoring systems. *The Scientific World Journal*. 2013;2013.

- [14] Carpinteri A, Lacidogna G, Accornero F, Mpalaskas AC, Matikas TE, Aggelis DG. Influence of damage in the acoustic emission parameters. *Cement and Concrete Composites*. 2013;44:9-16.
- [15] Carpinteri A, Pugno N. Fractal fragmentation theory for size effects of quasi-brittle materials in compression. *Magazine of Concrete Research*. 2005;57(6):309-313.
- [16] Klinkenberg B. A review of methods used to determine the fractal dimension of linear features. *International Association for Mathematical Geology*. 1994;26;No.1;23-46.
- [17] Landis EN, Baillon L, editors. Acoustic emission measurements of fracture energy. The fourth international conference on fracture mechanics of concrete and concrete structures; 2001; Cachan, France: A.A.BALKEMA PUBLISHERS.
- [18] Sagar RV, editor An experimental study on acoustic emission energy and fracture energy of concrete. National Seminar & Exhibition on Non-Destructive Evaluation; 2009; Tiruchirappalli, India.
- [19] Carpinteri A, Lacidogna G, Pugno N. Structural damage diagnosis and life-time assessment by acoustic emission monitoring. *Engineering Fracture Mechanics*. 2007;74(1-2):273-289.
- [20] Long M, Peng F. A Box-Counting Method with Adaptable Box Height for Measuring the Fractal Feature of Images. *Radioengineering*. 2013;22(1):208-213.
- [21] Nayak SR, Mishra J. An improved method to estimate the fractal dimension of colour images. *Perspectives in Science*. 2016;8:412-416.
- [22] Berke J, editor Spectral Fractal Dimension. The 4th WSEAS International Conference on Telecommunications and Informatics; 2005; Prague, Czech Republic.
- [23] Harrar K, Hamami L, editors. The box counting method for evaluate the fractal dimension in radiographic images. 6th WSEAS International Conference on Circuits, Systems, Electronics, Control & Signal Processing; 2007; Cairo, Egypt: WSEAS Press.
- [24] Reishofer G, Koschutnig K, Enzinger C, Ebner F, Ahammer H. Fractal dimension and vessel complexity in patients with cerebral arteriovenous malformations. *PLoS ONE*. 2012;7(7).
- [25] Panigrahy C, Garcia-Pedrero A, Seal A, Rodríguez-Esparragón D, Mahato NK, Gonzalo-Martín C. An approximated box height for Differential-Box-Counting method to estimate fractal dimensions of gray-scale images. *Entropy*. 2017;19(10).
- [26] Ritchie RO. Mechanisms of fatigue-crack propagation in ductile and brittle solids. *International Journal of Fracture*. 1999;100:55-83